# Catalytic performance of cement clinker supported nickel catalyst in glycerol dry reforming

Hua Chyn Lee[a],   Kah Weng Siew[a],   Maksudur R. Khan[a],   Sim Yee Chin[a,b],
Jolius Gimbun[a,b],   Chin Kui Cheng[a,b*]

a. Faculty of Chemical & Natural Resources Engineering, Universiti Malaysia Pahang, Lebuhraya Tun Razak, 26300 Gambang Kuantan, Pahang Malaysia;
b. Centre of Excellence for Advanced Research in Fluid Flow, Universiti Malaysia Pahang, Lebuhraya Tun Razak, 26300 Gambang Kuantan, Pahang Malaysia

## Abstract

The paper reports the development of cement clinker-supported nickel (with metal loadings of 5 wt%, 10 wt%, 15 wt% and 20 wt%) catalysts for glycerol dry ($CO_2$) reforming reaction. XRF results showed that CaO constituted 62.0% of cement clinker. The physicochemical characterization of the catalysts revealed 32-folds increment of BET surface area ($S_{BET}$) with the addition of nickel metal into the cement clinker, which was also corroborated by FESEM images. Significantly, XRD results suggested different types of Ni oxides formation with Ni loading, whilst $Ca_3SiO_5$ and $Ca_2Al_{0.67}Mn_{0.33}FeO_5$ were the main crystallite species for pure cement clinker. Temperature-programmed reduction analysis yielded three domains of $H_2$ reduction peaks, viz. centered at approximately 750 K referred to as type-I peaks, another peaks at 820 K denoted as type-II peaks and the highest reduction peaks, type-III recorded at above 1000 K. 20 wt% Ni was found to be the best loading with the highest $X_G$ and $H_2$ yield, whilst the lowest methanation activity. Syngas with lower $H_2/CO$ ratios (0.6 to 1.5) were readily produced from glycerol dry reforming at $CO_2$-to-Glycerol feed ratio (CGR) of unity. Nonetheless, carbon deposit comprised of whisker type ($C_v$) and graphitic-like type ($C_c$) species were found to be in majority on 20 wt%Ni/CC catalysts.

## Key words

cement clinker; dry reforming; glycerol; nickel catalyst; syngas

## 1. Introduction

The global energy consumption is expected to attain 820 quadrillion British thermal units (Btu) by the year 2040 from the current 524 quadrillion Btu [1]. If the same consumption pattern continues, 80% of the world energy usage will still depend on the fossil fuel. Unfortunately, fossil fuel combustion for transportation and electricity purposes is a major source of the anthropogenic carbon dioxide ($CO_2$) emission. $CO_2$ concentration in atmosphere has once surpassed 400 parts per million (ppm), a level deemed detrimental to climate change [2]. International agreement on limiting warming to 2 °C will only be achieved if two-third of the fossil fuel reserve remains underground by the year 2050 as reported in the 2012 IEA World Energy Outlook report [3]. Significantly, a combination of factors such as fossil fuel depletion and growing environmental concern have largely driven a search for more sustainable and renewable resources. In particular, for biomass-rich nation like Malaysia, the answer seems to be obvious. The Malaysian government has planned to fully implement B5 mandate (5% methyl ester in diesel) nationwide in July 2014. There were 60 biodiesel manufacturing licenses being approved by the government anticipating total annual biodiesel production of 6.5 MT. It is widely known that during the transesterification, 10 wt% glycerol bio-waste is obtained [4−7]. Therefore, an annual production of 0.6 MT of crude glycerol is anticipated. High impurity contents in the crude glycerol necessitate an expensive purification process [8–10]. This has confined the applications of purified glycerol to pharmaceutical, cosmetic and food industries. Hence finding alternative use of crude glycerol is significant. Conversion of glycerol (bio-waste) into biofuel or chemical products, i.e. syngas (mixture of $H_2$ and CO), acetone, acrolein, ethers and methanol [11−14], has been touted as a promising route to provide a total solution to the biodiesel industries, as well as energy sustainability.

Syngas is primarily being generated from natural gas, in particular methane ($CH_4$) reforming. Nonetheless, it is more enticing to derive syngas from glycerol biowaste instead as

glycerol ($C_3H_8O_3$) possesses more H-elements than $CH_4$. Glycerol steam reforming (Equation 1) has also been extensively studied over the past decade [15−17]. However, it produces high $H_2/CO$ ratios (typically more than 10) under excess steam conditions, as CO has undergone water-gas-shift (WGS) reaction (Equation 2) which is unfavourable for Fischer-Tropsch (FT) synthesis [18,19]. Another drawback of glycerol steam reforming is significant production of $CO_2$.

$$C_3H_8 + 6H_2O \rightarrow 3CO_2 + 10H_2 \tag{1}$$

$$CO + H_2O \rightarrow CO_2 + H_2 \tag{2}$$
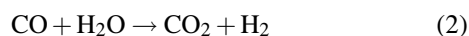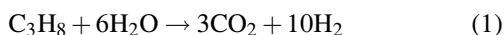
To mitigate $CO_2$ emission, dry ($CO_2$) reforming has gained popularity as an alternative to steam reforming. Dry reforming is highly selective to CO as compared with steam reforming, hence lower $H_2/CO$ ratio is more suitable for FT synthesis and methanol synthesis without syngas conditioning. Dry reforming has been extensively reported for methane, propane, ethanol and toluene [20–25], yet little works have been dedicated to glycerol dry reforming, which are limited to the thermodynamically study by Wang and his co-workers [26]. The overall glycerol dry reforming concept is expressed as in Equation (3).

$$C_3H_8O_3 + CO_2 \rightarrow 4CO + 3H_2 + H_2O \tag{3}$$
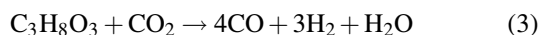
Nickel-based catalysts have widely replaced the noble catalysts such as Rh, Pt and Pd [27−29] in various reforming technologies due to their availability and lower costs. Ni-based catalysts possess high activity in hydrogenation and dehydrogenation, which means the bond cleavages between O−H, −CH$_2$−, C−C and −CH$_3$− are easily accomplished [30]. Nevertheless, it is well-known that Ni-based catalysts suffered from the deactivation attributed to coke deposition. Coke deposition is influenced by the types of support employed. Modification of catalyst support by addition of strong Lewis base oxide such as CaO and MgO has improved carbon deactivation resistance during reforming [31−33]. Previous studies [34,35] reported that cement clinker (CC) contains 63.28% and 63.17% CaO respectively, hence exhibiting properties suitable as catalyst synthesis. CC is an intermediate product of the cement industries. Halmann and Steinfeld [36] have performed the thermo-chemical calculations for the co-production of limestone (CaO) and syngas via $CH_4$ dry reforming, using $CO_2$ released from lime-kiln. Gimbun et al. [37] have activated CC for biodiesel production and glycerol was the by-product. Some of the researchers also reported that carbon nanotubes deposited on Ni catalyst could mechanical-strengthened the cementitious material. Therefore, it is feasible to conduct reforming of glycerol (from the biodiesel industry) over the CC utilizing the emitted $CO_2$ from the cement kiln. This will provide an utmost solution to environment, cement and biodiesel industry. The current work serves to characterize the catalysts using spectroscopic analysis and also to investigate the activity of glycerol dry reforming over CC-supported Ni catalysts with the aims of producing syngas and understanding the carbon laydown behaviour.

## 2. Experimental

### 2.1. Materials and catalyst preparation

Analytical grade glycerol was supplied by Sigma Aldrich and the CC was obtained from the Pahang Cement Sdn. Bhd. CC was ground with mortar and sieved for the particle range of 100−200 $\mu$m before wet-impregnated with 5 wt%, 10 wt%, 15 wt% and 20 wt% nickel (Ni)-metal, respectively, using $Ni(NO_3)_2 \cdot 6H_2O$ as precursor in 50 mL ultrapure water. Subsequently, the resulting slurry was stirred for 3 h at room temperature before oven-dried for 24 h at 403 K. The catalysts were then air-calcined at 1073 K for 6 h at 5 K·min$^{-1}$. Postcalcination, the catalysts were ground and sieved again to the size of 90−200 $\mu$m for reaction studies.

### 2.2. Catalyst characterization

$N_2$ physisorption isotherms of the catalysts were performed at 77 K using thermo scientific surface gas adsorption porosimeter. Before physisorption, the catalysts were degassed overnight at 573 K and $1 \times 10^{-4}$ Torr. The cumulative pore size was determined using Barett-Joyner-Halenda (BJH) equation. The oxide composition of the catalysts was determined by wavelength X-ray fluorescence (WD-XRF) spectrometry (Bruker, S8 Tiger Model, Germany). The crystalline behaviour of the catalysts was measured by powder XRD measurement (Rigaku Miniflex II) with Cu $K_\alpha$ radiation, $\lambda = 1.5418$ Å at 30 kV and 15 mA, from $2\theta$ of $10^o$ to $80^o$ with a step size of $0.02^o$ and a step time of 1 s. The oxide crystalline size of the catalysts was determined using Scherrer equation, $d = 0.94\lambda/(\beta_d \cos\theta)$, where $d$ is the crystallite size, $\lambda$ is the wavelength of the radiation, $\beta_d$ is the full-width at half maximum (FWHM) of the diffraction peak and $\theta$ is the half of the diffraction angle.

The surface structure of the catalysts was captured by field emission electron microscopy (FESEM) model JOEL/JSM-7800F, equipped with energy microscopy dispersive spectroscopy (EDS). Qualitatively, Fourier transform infrared (FTIR) spectra of the catalysts were recorded from 600 to 4000 cm$^{-1}$ with a Perkin Elmer (Model Spectrum 100) FTIR spectrophotometer using KBr disks technique. Thermogravimetric analysis (TGA) was performed to observe the gas-solid catalyst interaction in 60 mL·min$^{-1}$ of air with 40 mL·min$^{-1}$ of $N_2$ carrier up to 1173 K employing ramping rate of 10 K·min$^{-1}$.

Temperature-programmed reduction (TPR) was performed using Thermo Finnigan TPD/R/O 1100 series unit equipped with TCD detector to gauge the reducibility of the catalysts. An approximately 0.1 g catalyst (with different Ni loadings) was reduced with 20 mL·min$^{-1}$ 5% $H_2$ in $N_2$ carrier gas at ramping 20 K·min$^{-1}$ up to 1173 K with holding period of 30 min prior to cooling to room temperature.

After the reaction, temperature-programmed oxidation (TPO) and FESEM were also performed on the used catalysts to examine the carbon deposition phenomenon and types